

# Technical Correspondence

## Elman Fuzzy Adaptive Control for Obstacle Avoidance of Mobile Robots Using Hybrid Force/Position Incorporation

Shuhuan Wen, Wei Zheng, Jinghai Zhu, Xiaoli Li, and Shengyong Chen

**Abstract**—This paper addresses a virtual force field between mobile robots and obstacles to keep them away with a desired distance. An online learning method of hybrid force/position control is proposed for obstacle avoidance in a robot environment. An Elman neural network is proposed to compensate the effect of uncertainties between the dynamic robot model and the obstacles. Moreover, this paper uses an Elman fuzzy adaptive controller to adjust the exact distance between the robot and the obstacles. The effectiveness of the proposed method is demonstrated by simulation examples.

**Index Terms**—Elman neural network (ENN), fuzzy PD control, hybrid force/position control, mobile robot, obstacle avoidance, path planning.

### I. INTRODUCTION

Mobile robots have been widely applied in many modern applications [1], [2]. The newly developed robots can complete very complicated tasks by improving adaptive ability of the robot system. This kind of robots is currently an important research topic. The basic feature of mobile robots is to possess the obstacle avoidance capability, which is inherently one of the most difficult tasks in path planning.

Obstacle avoidance control can be classified into motion control and dynamic control according to whether its controller considers dynamic properties of the robot [3], [4]. Many avoidance algorithms were developed by the model of mobile robot kinematics, while ignoring its dynamic behavior. Meanwhile, utilizing insufficient position control only to deal with dynamic interactional obstacle, a control algorithm has been introduced to describe the dynamic relationship between the mobile robot and moving objects. Force control was implemented by a proportional integral derivative (PID) controller in the early stage [5]. Recently, the advanced adaptive control method [6] and robust method [7], [8] have been devised. Typical algorithms include sliding mode control [9], [10], fuzzy control [11], [12], and neural network methods [13], [14]. The force control system usually involves either ability/location, or speed/position hybrid control [15]–[17] and impedance control [18].

Manuscript received December 20, 2010; revised March 28, 2011; accepted May 8, 2011. Date of publication June 23, 2011; date of current version June 13, 2012. This work was supported by the National Natural Science Foundation of China under 61025019, 60870002, and R1110679, and Natural Science Foundation of Hebei China under F2009001638. This paper was recommended by Associate Editor X. Guan.

S. Wen, W. Zheng, J. Zhu, and X. Li are with the Key Lab of Industrial Computer Control Engineering of Hebei Province, Yanshan University, Qinhuangdao 066004, China (e-mail: wenshuhuan@sohu.com; xiaoxiong19871110@163.com; zjh1632006@163.com; xiaoli.avh@gmail.com).

S. Chen (corresponding author) is with the College of Computer Science, Zhejiang University of Technology, Hangzhou 310023, China (e-mail: sy@ieee.org).

Color versions of one or more of the figures in this paper are available online at <http://ieeexplore.ieee.org>.

Digital Object Identifier 10.1109/TSMCC.2011.2157682

In this paper, a new method is proposed for mobile robots based on the Elman neural network (ENN) algorithm and fuzzy obstacle avoidance. A virtual force field is described between the robot and obstacles by the hybrid force algorithm. It is expected that the hybrid force/position control can realize online collision avoidance in a complex environment with many static and dynamic obstacles. In the previous work, the performance of obstacle avoidance methods is usually not satisfactory because the model of robotic dynamics is not accurate enough. Researchers have also attempted neural network compensation methods [19], [20]. However, the achieved result is limited in practical applications. In this paper, we first adopt ENN to compensate for uncertainty, while a number of shortcomings will be brought up with ENN alone to control the system, for example, real-time difference and relatively strong dependence on the hardware. Therefore, neural network-based fuzzy algorithms are then employed to realize online self-tuning and to reduce the influence of uncertainties during the control. It is expected that the fuzzy control combined with a neural network can achieve a better control performance than previous methods, i.e., the enhancement of the obstacle avoidance capability of mobile robots. Finally, some simulation experiments are carried out with a wheeled mobile robot to verify the effectiveness of the proposed method for obstacle avoidance control.

### II. MATHEMATICAL MODEL OF WHEELED ROBOTS

Generally, while a mobile robot moves on the plane, its dynamic model depends rather on the potential energy than on the dynamic energy [21]. Therefore, its model can be described as

$$M(q)\ddot{q} + C(q, \dot{q}) = P(q)\tau - A^T(q)\lambda \quad (1)$$

where  $q$  is the position vector for mobile robot,  $M(q)$  is an inertial matrix,  $C(q, \dot{q})$  is the centrifugal and Coriolis forces,  $P(q)$  is the input matrix,  $\tau$  is the moment vector,  $A(q)$  is the Jacobian matrix, and  $\lambda$  is the Lagrange factor. The parameters of robot's dynamics are

$$\tau = \begin{bmatrix} \tau_R \\ \tau_L \end{bmatrix} \quad (2)$$

$$M(q) = \begin{bmatrix} m & 0 & -m_c d \sin \phi & 0 & 0 \\ 0 & m & m_c d \cos \phi & 0 & 0 \\ -m_c d \sin \phi & m_c d \sin \phi & I & 0 & 0 \\ 0 & 0 & 0 & I_w & 0 \\ 0 & 0 & 0 & 0 & I_w \end{bmatrix} \quad (3)$$

$$P(q) = \begin{bmatrix} 0 & 0 \\ 0 & 0 \\ 0 & 0 \\ I & 0 \\ 0 & I \end{bmatrix} \quad C(q, \dot{q}) = \begin{bmatrix} -m_c d \dot{\theta}^2 \cos \phi \\ -m_c d \dot{\theta}^2 \sin \phi \\ 0 \\ 0 \\ 0 \end{bmatrix} \quad (4)$$

where  $m_c$  is the quality of mobile robot with no wheels,  $m$  is the mobile robot's total quality,  $I_w$  is the moment of  $\phi$ , and  $I$  is the moment of two wheels.

We can eliminate the Lagrange factor to make (1) much simpler. Then, the speed vector of the mobile robot is

$$\dot{q} = W(q)\dot{v}(t) \quad (5)$$

$$\dot{v}(t) = \begin{bmatrix} \dot{\theta}_R \\ \dot{\theta}_L \end{bmatrix} \dot{q} = \begin{bmatrix} \dot{y} \\ \dot{\phi} \\ \dot{\theta}_R \\ \dot{\theta}_L \end{bmatrix}. \quad (6)$$

We use matrix  $W^T$  which is mentioned earlier to eliminate the Lagrange factor, and the substitution of (5) into (1) yields

$$M(\dot{W}\dot{v}(t) + W\ddot{v}(t)) + C(q, \dot{q}) = P(q)\tau - A^T\lambda. \quad (7)$$

Since  $W^T A^T \lambda = 0$ , multiplying both sides of (7) by  $W^T$  we get

$$W^T [M(\dot{W}\dot{v}(t) + W\ddot{v}(t)) + C(q, \dot{q})] = W^T P\tau. \quad (8)$$

Furthermore,  $W^T P\tau = \tau$ ; we can, therefore, rewrite (8) as

$$W^T M\dot{W}\dot{v}(t) + W^T MW\ddot{v}(t) + W^T C(q, \dot{q}) = \tau. \quad (9)$$

For the matrix  $W$  mentioned earlier, we can use the following equation to make sure  $W^T A^T \lambda = 0$ :

$$W(q) = \begin{bmatrix} \frac{r}{2\cos\phi} - \frac{r}{l}(d\sin\phi + a\cos\phi) & \frac{r}{2\cos\phi} + \frac{r}{l}(d\sin\phi + a\cos\phi) \\ \frac{r}{2\sin\phi} + \frac{r}{l}(d\cos\phi - a\sin\phi) & \frac{r}{2\sin\phi} - \frac{r}{l}(d\cos\phi - a\sin\phi) \\ \frac{r}{l} & -\frac{r}{l} \\ 1 & 0 \\ 0 & 1 \end{bmatrix}. \quad (10)$$

By substitution of (10) into (9) and after simplification, we get the equations of system dynamics as follows:

$$\begin{bmatrix} D_{11} & D_{12} \\ D_{21} & D_{22} \end{bmatrix} \begin{bmatrix} \ddot{\theta}_R \\ \ddot{\theta}_L \end{bmatrix} + \begin{bmatrix} 2c^3bd(m+m_c)(\dot{\theta}_R\dot{\theta}_L - \dot{\theta}_L^2) \\ 2c^3bd(m+m_c)(\dot{\theta}_R\dot{\theta}_L - \dot{\theta}_R^2) \end{bmatrix} = \begin{bmatrix} \tau_R \\ \tau_L \end{bmatrix}$$

$$\begin{aligned} D_{11} &= c^2m(b^2 + d^2) + 2c^2d^2m_c + c^2I + I_w \\ D_{12} &= c^2[m(b^2 - d^2) - 2d^2m_c - I] \\ D_{21} &= c^2[m(b^2 - d^2) - 2d^2m_c - I] \\ D_{22} &= c^2m(b^2 + d^2) + 2c^2d^2m_c + c^2I + I_w \end{aligned} \quad (11)$$

where  $b \equiv l/2$ , and  $c \equiv r/l$ .

Suppose the robot moves slowly on the plane (which is true in most real cases); then, the centrifugal and Coriolis forces will equal zero. From this fact, we can finally make the dynamic model much simpler as

$$\begin{bmatrix} D_{11} & D_{12} \\ D_{21} & D_{22} \end{bmatrix} \begin{bmatrix} \ddot{\theta}_R \\ \ddot{\theta}_L \end{bmatrix} = \begin{bmatrix} \tau_R \\ \tau_L \end{bmatrix}. \quad (12)$$

From the previous formulation, the mobile robot on the plane can be treated as a reduced inertia system. This is the reason why most mobile robots are based on the kinetic model. To model wheeled robots, we can first start from the kinetic model by obtaining the definition of Lagrange matrix, and then obtain the motion model and matrix model of the wheeled robot based on the dynamic model of ordinary robots.

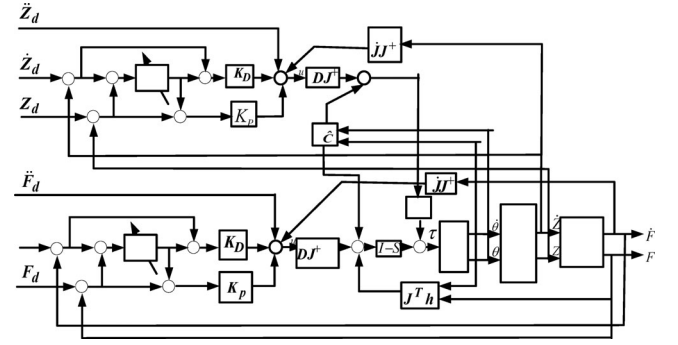


Fig. 1. Block diagram of the Elman fuzzy self-adaption hybrid force/position control.

### III. ELMAN FUZZY SELF-ADAPTION AND HYBRID FORCE/POSITION CONTROL

It is difficult to apply an explicit robot model because there are many uncertain factors in the environment. It is always limited if we use one fuzzy proportional derivative (PD) controller only to adjust errors. In order to optimize the control performance, we introduce an intelligent regulation, i.e., ENN control, for compensation.

The compensating signals that we get from ENN control can be added into the input of a fuzzy PD regulator to reduce output errors. This can compensate the system uncertainty, while not affecting the interior structure of the control system. There are six inputs and one output in the ENN. They serve different roles in control of the position direction and the force direction. The output compensating signals are also added into the input for position and force control, correspondingly. For control of the force direction, we have the inputs

$$\ddot{F} = \ddot{F}_d + K_D(\dot{F}_d - \dot{F}) + K_P(F_d - F + \Phi_f) \quad (13)$$

where  $\Phi_f$  is the compensating signal from the ENN.

We can get the control law as follows by the substitution of (14) into (15):

$$\begin{aligned} f_x &= k_e \delta_x \\ f_y &= k_e \delta_y \end{aligned} \quad (14)$$

$$u_2 = \ddot{z} = \ddot{z}_d + k_D(\dot{z}_d - \dot{z}) + k_P(z_d - z) \quad (15)$$

$$\begin{aligned} \tau &= \hat{D}J^+ K_e^{-1}[\ddot{F}_d + K_D(\dot{F}_d - \dot{F}) + K_P(F_d - F + \Phi_f) \\ &\quad - \hat{J}J^+ K_e^{-1}\dot{F}] + \hat{C} + J^T h. \end{aligned} \quad (16)$$

For the position direction, we use the following control law:

$$\ddot{Z} = \ddot{Z}_d + K_D(\dot{Z}_d - \dot{Z}) + K_P(Z_d - Z + \Phi_P). \quad (17)$$

The block diagram of the Elman fuzzy self-adaption hybrid force/position control is illustrated in Fig. 1.

The synthetic control law is

$$\begin{aligned} \tau &= S\{\hat{D}J^+ [\ddot{Z}_d + K_D(\dot{Z}_d - \dot{Z}) - \hat{J}J^+ \dot{Z} + K_P(Z_d - Z + \Phi_P)] + \hat{C}\} \\ &\quad + (1-S)\{\hat{D}J^+ K_e^{-1}[\ddot{F}_d + K_D(\dot{F}_d - \dot{F}) + K_P(F_d - F + \Phi_f) \\ &\quad - \hat{J}J^+ K_e^{-1}\dot{F}] + \hat{C} + J^T h\}. \end{aligned} \quad (18)$$

Here

$$K_e = \begin{bmatrix} k_e & 0 & 0 \\ 0 & k_e & 0 \\ 0 & 0 & 1 \end{bmatrix} \quad \text{and} \quad K_P = \begin{bmatrix} K_{PX} & 0 & 0 \\ 0 & K_{PY} & 0 \\ 0 & 0 & K_{P\Phi} \end{bmatrix}.$$

TABLE I  
BASIC PARAMETERS

|     |        |       |          |       |         |       |        |
|-----|--------|-------|----------|-------|---------|-------|--------|
| $r$ | $0.3m$ | $m$   | $0.13kg$ | $I_w$ | $0.2Nm$ | $f_1$ | $9.2N$ |
| $l$ | $0.5m$ | $m_c$ | $0.5kg$  | $I$   | $3Nm$   | $f_2$ | $8.7N$ |
| $d$ | $0.2m$ |       |          | $u$   | $2Nm$   |       |        |

TABLE II  
VALUES OF POSITION AND FORCE INPUT SIGNALS

|       |         |          |         |
|-------|---------|----------|---------|
| $x_d$ | 2       | $f_{xd}$ | 2       |
| $y_d$ | 2       | $f_{yd}$ | 2       |
| $i_d$ | $\pi/4$ | $f_{id}$ | $\pi/4$ |

TABLE III  
PARAMETERS OF THE CONTROLLER

|               |      |               |    |
|---------------|------|---------------|----|
| $k_{px}$      | 3000 | $k_{dx}$      | 80 |
| $k_{py}$      | 2000 | $k_{dy}$      | 60 |
| $k_{p\theta}$ | 1000 | $k_{d\theta}$ | 15 |

## IV. EXPERIMENTS AND RESULTS

First, we consider the mixed force control in the position direction. The mobile robots move along the expected trajectory in the positional direction. They can keep the desired distance in the direction of force control by using the virtual force. This paper combines two methods, i.e., conventional PD control and Elman Fuzzy control. By the use of the S-function in simulations, two control strategies are compared in the experiments.

Parameters of simulation and input signals are shown in Table I, where  $r$  is the wheel radius of a robot,  $l$  is the distance between the robot's two wheels,  $d$  is the distance from the midpoint of the axle to the focus of the robot,  $m$  and  $m_c$  are the all-up weight of the robot and the weight of the nonwheel robot, respectively,  $I_w$  is the torque of palstance  $\phi'$  that is the direction of advance, and  $I$  is the torque of two wheels. Here, input signal parameters of the external force and the torque include  $f_1$  that is the horizontal component of the external force,  $f_2$  that is the vertical component of the external force, and  $u$  that is the torque of the external force.

Typical values of positions and forces are given in Table II and the controller parameters are set in Table III. The positional conditions are organized as a vector, namely,  $z_d = [x_d \ y_d \ \phi_d]$ , where  $x_d$  is the abscissa,  $y_d$  is the ordinate, and  $\phi_d$  is the direction of the advance angle of the mobile robot. For the input force signal, these three variables represent the virtual force components in the directions of  $x$  and  $y$ , and its direction of the advance angle.

Here, we further explain the ENN input and output signals. In the direction of the position control,  $e_x = x_d - x$ ,  $e_y = y_d - y$ ,  $e_i = i_d - i$  where  $x$ ,  $y$ , and  $i$  are the three variables of the actual distances of the robot. They represent the obstacle in the  $x$ - and  $y$ -directions, and the actual direction of the advance angle. Taking  $e_x$ ,  $e_y$ ,  $e_i$ ,  $\dot{e}_x$ ,  $\dot{e}_y$ , and  $\dot{e}_i$  as the inputs and taking  $\Phi_p$  as the output, we can compensate the position error by the use of an ENN.

On the direction of force control,  $e_{fx} = f_{xd} - f_x$ ,  $e_{fy} = f_{yd} - f_y$ , and  $e_i = f_{id} - f_i$  where  $f_x$ ,  $f_y$ , and  $f_i$  represent three variables, i.e.,

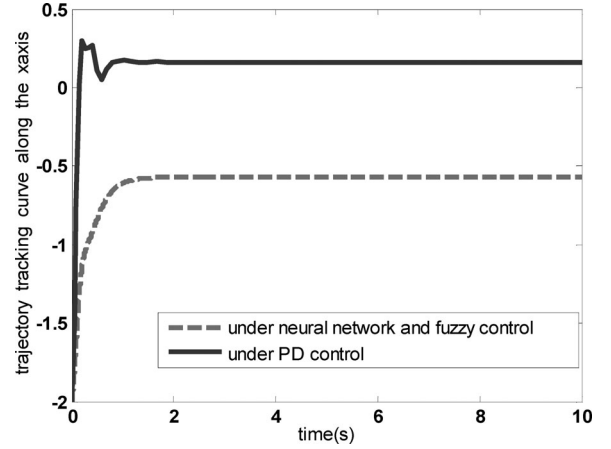


Fig. 2. X path trace of the curve.

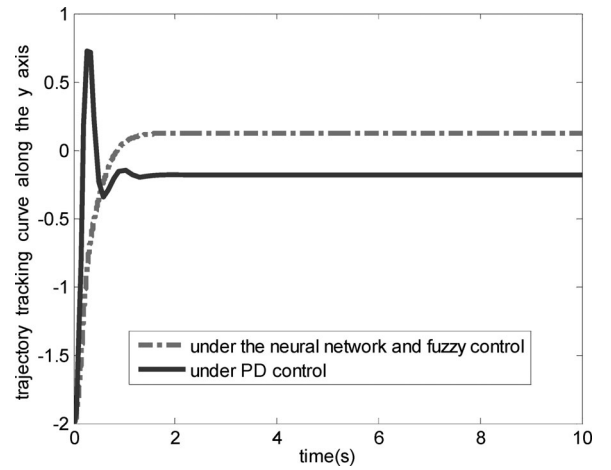


Fig. 3. Y path trace of the curve.

actual components of virtual force in the  $x$ - and  $y$ -directions between mobile robot and obstacle, and its direction of the advance angle. In the experiments, we take  $e_{fx}$ ,  $e_{fy}$ ,  $e_{fi}$ ,  $\dot{e}_{fx}$ ,  $\dot{e}_{fy}$ , and  $\dot{e}_{fi}$  as the inputs and take compensation signal  $\phi_f$  as the output. The ENN is established to compensate the force error signal. By doing so, we can compare and simulate the obstacle avoidance control by the use of Elman Fuzzy PD control and PD mixed force/position control.

## A. Path Tracking of Positional Vectors

Fig. 2 illustrates the simulation curve to infer the conclusion path tracing control. We use the Elman Fuzzy adaptive control and Elman track to trajectory. The result shows that control performance is significantly improved as the error almost reaches zero.

Fig. 3 illustrates another simulation curve. By the employment of ENNs and fuzzy adaptive control in the system, the error is greatly reduced or even eliminated. At the same time, the adjusting time is also gradually decreased. These experiments show that the robot successfully tracks the desired trajectory. In Fig. 4, the simulation curve shows that with the decrease in amplitude fluctuations, the stability becomes strengthened.

## B. Force Vector Errors

Fig. 5 illustrates the simulation curve by the use of the Elman fuzzy adaptive control in the system. From the figure, we can see that the

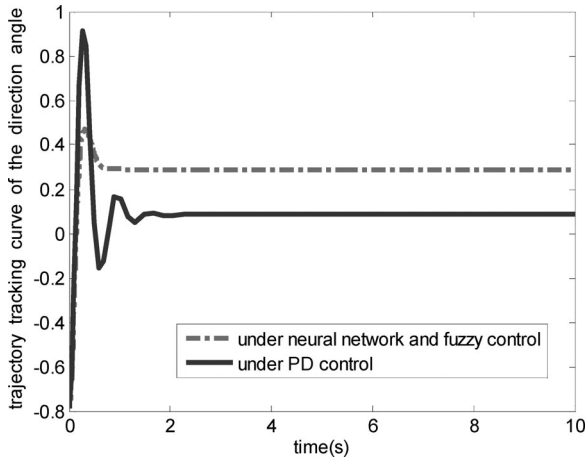


Fig. 4. Trajectory tracking curve of the direction angle.

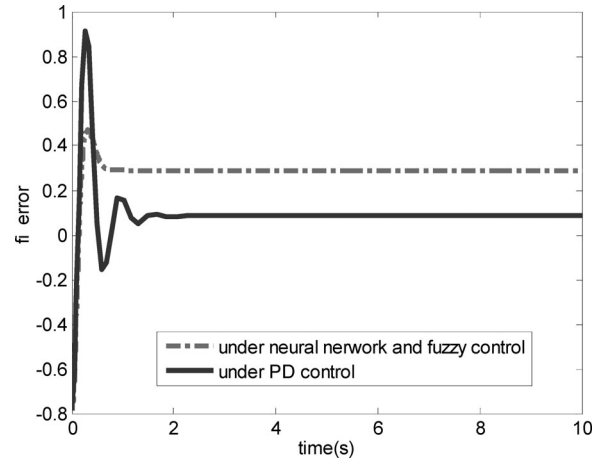
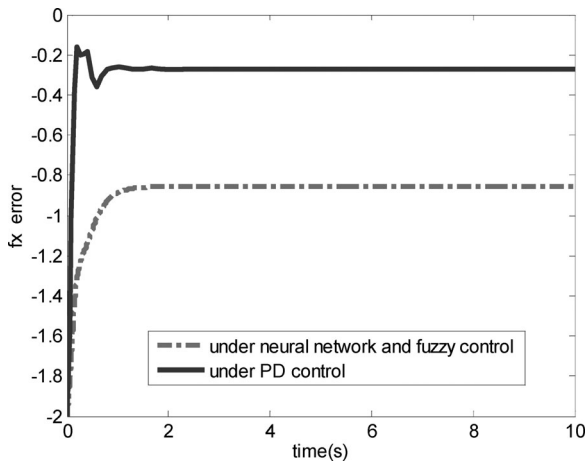
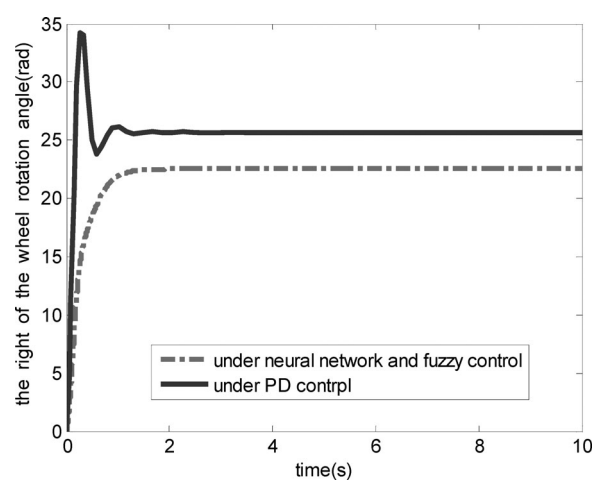
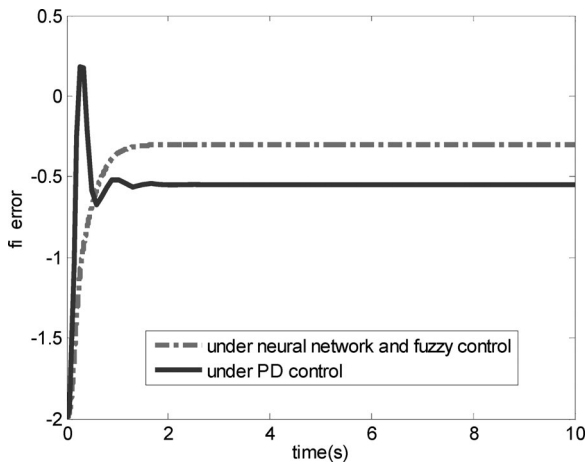
Fig. 7.  $F_i$  error.Fig. 5.  $F_x$  error.

Fig. 8. Left wheel rotation angle.

Fig. 6.  $F_y$  error.

horizontal component of the error curve in  $f_x$  precision is dramatically improved. The  $F_y$  error remains zero, while the time of the transition process is also reduced. The system shows good dynamic performance as the mobile robot displays a good ability to avoid obstacles.

In Figs. 6 and 7, there are the error curve overshoots and a steady-state error in the conventional PD control. The steady-state error size is

0.6 which cannot be ignored. When using ENN and fuzzy PD control system, the error overshoot quantity curve becomes much smaller. It also means that the mobile robot has a good ability to avoid obstacles.

### C. Wheel Rotation Angles

The wheels of the robot rotation curve reflect the characteristics of a mobile robot. Comparing Fig. 8 with the control of conventional PD, the results show that the rotation angle of the robot left wheel gives large fluctuation amplitude and unstable undulates. The same result is also shown by comparing with Fig. 9, which represents the rotation angle of the robot's right wheel.

Three-dimensional maps are provided here when using the Elman fuzzy adaptive control and conventional PD control. Figs. 10–13 show the corresponding obstacle avoidance. It can be found by comparing the avoidance performance between a single obstacle and two simultaneously. It is more accurate when using Elman fuzzy adaptive control because the curve is smoother, and the avoidance performance is better. The results also show that with one and two obstacles, the Elman fuzzy adaptive control algorithm can successfully avoid obstacles, and the moving speed is consistent. The proposed method can provide a controlling way with the effectiveness and efficiency to avoid multiple obstacles, by the consideration of both rapidity and stability. The task may be in arbitrary different environments and have different goals.

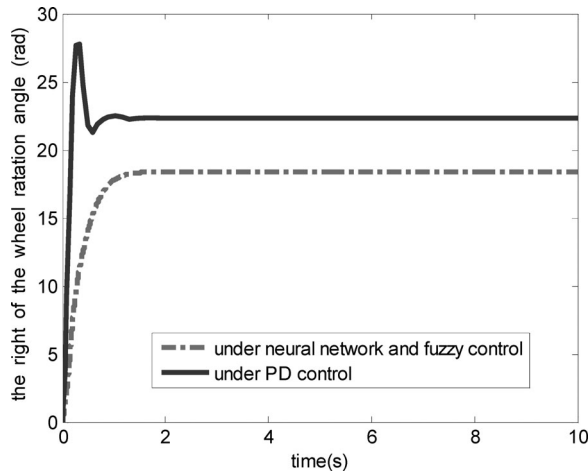


Fig. 9. Right wheel rotation angle.

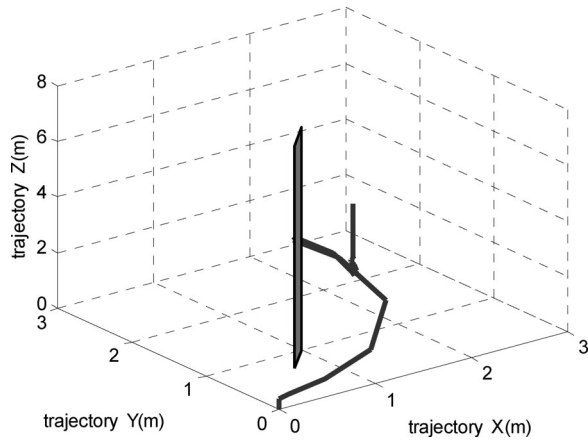


Fig. 10. PD control for collision avoidance of one obstacle.

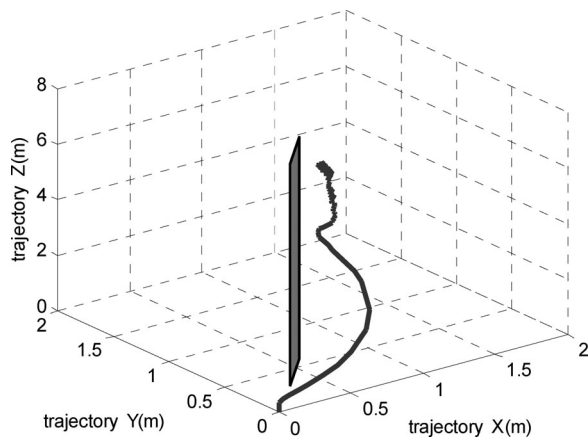


Fig. 11. ENN and fuzzy control for collision avoidance of one obstacle.

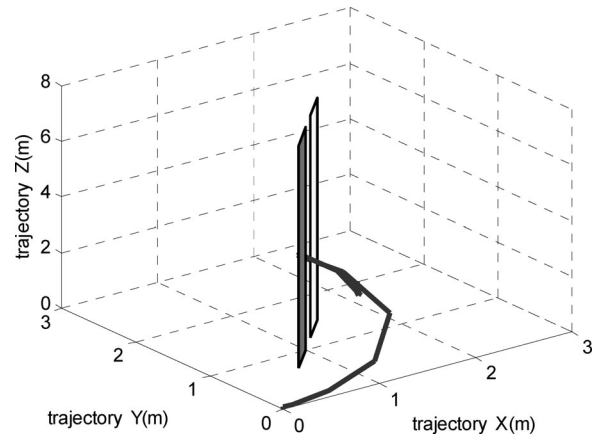


Fig. 12. PD control for two obstacles.

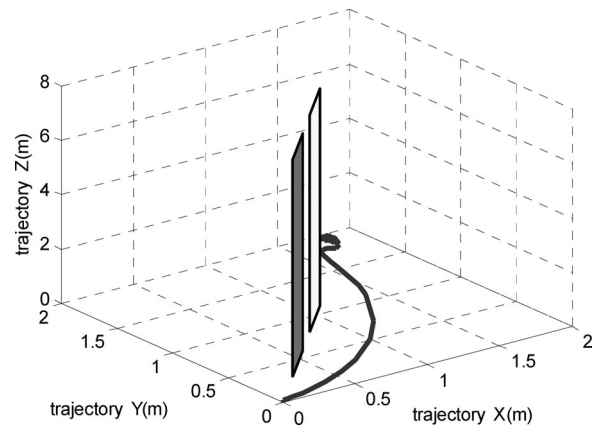


Fig. 13. ENN and fuzzy control for two obstacles.

## V. CONCLUSION

An ENN-Fuzzy controller has been designed in this paper for mobile robots. A novel collision avoidance algorithm has been developed by the utilization of a virtual force. The robot is planned to find its shortest path to the goal and at the same time maintains a desired distance from the obstacles. Dynamic behaviors of a mobile robot have been considered when it detects obstacles. The online ENN-Fuzzy control method can compensate for uncertainties in robotic dynamics. Experiments are carried out to compare tracking performance of PD control and ENN-Fuzzy control under uncertain environments. The results show that the ENN-Fuzzy method is a reliable control tool. It can capture and track the system's trajectory quickly and accurately.

## REFERENCES

- [1] M. A. Sharbafi, C. Lucas, and R. Daneshvar, "Motion control of omnidirectional three-wheel robots by brain-emotional-learning-based intelligent controller," *IEEE Trans. Syst., Man, Cybern., Part C*, vol. 40, no. 6, pp. 630–638, Nov. 2010.
- [2] A. Zhu and S. X. Yang, "Neurofuzzy-based approach to mobile robot navigation in unknown environments," *IEEE Trans. Syst., Man, Cybern., Part C*, vol. 37, no. 4, pp. 610–621, Jul. 2007.
- [3] H. Li, S. X. Yang, and M. L. Seto, "Neural-network-based path planning for a multirobot system with moving obstacles," *IEEE Trans. Syst., Man, Cybern., Part C*, vol. 39, no. 4, pp. 410–419, Jul. 2009.
- [4] M. Mucientes, R. Iglesias, C. V. Regueiro, A. Bugarin, P. Carinena, and S. Barro, "Fuzzy temporal rules for mobile robot guidance in dynamic environments," *IEEE Trans. Syst., Man, Cybern., Part C*, vol. 31, no. 3, pp. 391–398, Aug. 2001.



- [5] L. Zollo, B. Siciliano, A. De Luca, E. Guglielmelli, and P. Dario, "Compliance control for an anthropomorphic robot with elastic joints: Theory and experiments," *J. Dyn. Syst., Meas. Control*, vol. 127, no. 3, pp. 321–328, 2006.
- [6] J. Roy and L. L. Whitcomb, "Adaptive force control of position/velocity controlled robots: Theory and experiment," *IEEE Trans. Robots Autom.*, vol. 18, no. 2, pp. 121–137, Apr. 2001.
- [7] C. Chiu and K. Y. Lian, "Adaptive motion/force tracking control of holonomic constrained mechanical systems: A unified viewpoint," *Int. J. Adaptive Control Signal Process.*, vol. 21, pp. 415–433, 2007.
- [8] R. G. Landers, A. G. Ulsoy, and Y. H. Ma, "A comparison of model-based machining force control approaches," *Int. J. Mach. Tools Manufacture*, vol. 44, pp. 733–748, 2004.
- [9] M. Jerouane, N. Sepehri, and F. Lamnabhi-Lagarigue, "Dynamic analysis of variable structure force control of hydraulic reaching law approach," *Int. J. Control*, vol. 77, pp. 1260–1268, 2004.
- [10] V. Parra-Vega, A. Rodríguez-Angeles, and G. Hirzinger, "Perfect position/force tracking of robots with dynamical terminal control," *J. Robot. Syst.*, vol. 18, pp. 517–532, 2001.
- [11] Y. Fu, H. Li, and M. E. Kaye, "Hardware/software codesign for a fuzzy autonomous road-following system," *IEEE Trans. Syst., Man, and Cybern., Part C*, vol. 40, no. 6, pp. 690–696, Nov. 2010.
- [12] L. Birglen and C. M. Gosselin, "Fuzzy enhanced control of an underactuated finger using tactile and position sensors," in *Proc. IEEE Int. Conf. Robot. Autom.*, 2005, vol. 15, no. 4, pp. 2320–2325.
- [13] A. Fanaci and M. Farrokhi, "Robust adaptive neuro-fuzzy controller for hybrid position/force control of robot manipulators in contact with unknown environment," *J. Intell. Fuzzy Syst.*, vol. 17, pp. 125–144, 2006.
- [14] V. Mallapragada, D. Erol, and N. Sarkar, "A new method of force control for unknown environments," in *Proc. IEEE Int. Conf. Intell. Robots Syst.*, 2006, vol. 6, pp. 4509–4514.
- [15] O. Chuy, Y. Hirata, and K. Kosuge, "A new control approach for a robotic walking support system in adapting user characteristics," *IEEE Trans. Syst., Man, Cybern., Part C*, vol. 36, no. 6, pp. 725–733, Nov. 2006.
- [16] C. Q. Huang, S. J. Shi, X. G. Wang, and W. K. Chung, "Parallel force/position controls for robot manipulators with uncertain kinematic," *Int. J. Robot. Autom.*, vol. 20, pp. 158–168, 2005.
- [17] G. Ziliani, A. Visioli, and G. Legnani, "Gain scheduling for hybrid force/velocity control in contour tracking task," *Int. J. Adv. Robot. Syst.*, vol. 3, pp. 367–374, 2006.
- [18] S. G. Wysoski, L. Benuskova, and N. Kasabov, "Evolving spiking neural networks for audiovisual information processing," *Neural Netw.*, vol. 23, pp. 819–835, 2010.
- [19] F. Zhang, Y. Xi, Z. Lin, and W. Chen, "Constrained motion model of mobile robots and its applications," *IEEE Trans. Syst., Man, Cybern.*, vol. 39, no. 3, pp. 773–787, Jun. 2009.
- [20] B. Marwin, F. Simon, and C. Liberato, "Dual adaptive dynamic control of mobile robots using neural networks," *IEEE Trans. Syst., Man, Cybern.*, vol. 39, no. 1, p. 129–141, Feb. 2009.
- [21] S. Jung, E. S. Jang, and T. C. Hsia, "Collision avoidance of a mobile robot using intelligent," in *Proc. Int. Conf. Robot. Autom.*, 2005, vol. 8, pp. 4418–4423.